

AVOIDING TRAPS IN NONCONVEX PROBLEMS

SEAN DEYO^{1,*}, VEIT ELSER¹

¹*Department of Physics, Cornell University, Ithaca, NY, USA*

Abstract. Iterative projection methods may become trapped at non-solutions when the constraint sets are nonconvex. Two kinds of parameters are available to help avoid this behavior and this study gives examples of both. The first kind of parameter, called a hyperparameter, includes any kind of parameter that appears in the definition of the iteration rule itself. The second kind comprises metric parameters in the definition of the constraint sets, a feature that arises when the problem to be solved has two or more kinds of variables. Through examples we show the importance of properly tuning both kinds of parameters and offer heuristic interpretations of the observed behavior.

Keywords. Projection methods; Fixed-point algorithms; Nonconvex problems; Logical satisfiability; Dominating sets; Machine learning.

1. INTRODUCTION

Iterative algorithms whose elementary operations are projections to constraint sets perform well on many nonconvex problems for which one does not have the convergence guarantees one has in convex problems. For some combinatorially hard problems these algorithms routinely outperform state-of-the-art algorithms that find solutions by exhaustive search [1]. This success, or the apparent ability of the projection-based search to very significantly reduce the size of the space being searched, is poorly understood.

The standard criteria for evaluating iterative projection algorithms in the convex case do not apply in the nonconvex case. The amount of time the algorithm spends refining a solution, once its locally convex basin has been encountered, is negligible compared to the time needed to find the basin. Efficiency in basin discovery completely overshadows the benefits of good convergence within the basin.

Iterative projection algorithms usually follow a fixed-point principle, where fixed-points imply a solution, but these algorithms may still get trapped on non-solutions in a dynamic sense [2]. When this happens, the iterations meander indefinitely within a small domain far from a true fixed point. Eliminating or mitigating this behavior by tuning the parameters of the algorithm is the focus of this paper.

Most iterative projection algorithms have parameters that apply to the general case, independent of the application's constraint sets. For such parameters we use the machine learning term "hyperparameter." Relaxation parameters are examples of hyperparameters. Another type of parameter has only come to light more recently, in applications that require multiple kinds of variables [3]. These applications have variable-scaling freedom that is not a geometrical isometry and therefore changes the algorithm through its effect on the projections. We refer to such parameters as "metric parameters."

*Corresponding author.

E-mail addresses: sjd257@cornell.edu (S. Deyo), ve10@cornell.edu (V. Elser).

Submitted June 10, 2021

2. HYPERPARAMETERS AND METRIC PARAMETERS

One of the best known hyperparameters is the relaxation that is often applied to the Douglas-Rachford iteration [4]

$$x \mapsto (1 - \beta/2)x + (\beta/2)R_B(R_A(x)). \quad (2.1)$$

Here R_A and R_B are the reflectors for the constraint sets A and B . The hyperparameter β is the same parameter that independently was deemed important when this iteration was proposed — by an engineer unaware of Douglas-Rachford — for the phase retrieval application [5]. To make the point that the scope of hyperparameters is broad, we give an example in section 3 of a very different generalization of Douglas-Rachford, in which tuning a hyperparameter is critical for success.

In imaging applications [6], or even sudoku [7], where there is just one kind of pixel or cell, the question of metric parameters never came up. An application where introducing metric parameters makes sense is non-negative matrix factorization (NMF) [8]. In NMF one seeks a low-rank factorization of a rectangular non-negative matrix $Z = XY$, where the factors are themselves non-negative. The rows of Z may be interpreted as data vectors that can be expressed as non-negative mixtures, given by X , of a set of non-negative features, the rows of Y . NMF is non-unique with respect to rescaling ($X \rightarrow XD, Y \rightarrow D^{-1}Y$, arbitrary diagonal and positive D). To remove this ambiguity and also to make the problem compact, we can choose to impose a norm on the columns of X or the rows of Y . If we decide to normalize the features (Y), what setting of the norm do we choose and why is that a choice of metric?

To motivate the term “metric,” consider the standard distance that would be used in defining the projections for the NMF application:

$$d((X, Y), (X', Y')) = \sqrt{\|X - X'\|_2^2 + \|Y - Y'\|_2^2}. \quad (2.2)$$

Now, if we chose to impose normalization on each row vector y of Y , say $\|y\|_2 = \eta$, we could alternatively work with the rescaled variables $\tilde{Y} = Y/\eta$, normalization constraint $\|\tilde{y}\|_2 = 1$, and the distance

$$d((X, \tilde{Y}), (X', \tilde{Y}')) = \sqrt{\|X - X'\|_2^2 + \eta^2 \|\tilde{Y} - \tilde{Y}'\|_2^2}. \quad (2.3)$$

This rewriting by a parameterized distance provides an interpretation of the norm parameter η . Consider the projection to the bilinear constraint, $X\tilde{Y} = Z/\eta$. From the distance (2.3) we see that for small η the \tilde{Y} variables (features) are more compliant than X (mixtures), and we should expect that product-constraint inconsistencies are resolved mostly by changing the features. The opposite, or more reliance on changing the mixtures, is expected for large η .

NMF is one of the earliest techniques of machine learning, and we anticipate that variable-type metric sensitivity will grow in relevance as projection methods find their way into this domain¹. In particular, splitting methods lend themselves naturally to optimization on networks, where variables appear on both nodes and edges of the network and are clearly dissimilar.

1. The term “parameter” is potentially confusing in the machine learning context. For example, the *weight parameters* of a neural network that are learned from data are variables from the perspective of the optimization algorithm. The latter may use *metric parameters* to more efficiently optimize the *weight variables*.

3. HYPERPARAMETERS

A tuneable double-reflector algorithm. In this section we consider a generalization of the Douglas-Rachford iteration that is very different from the standard relaxation (2.1) :

$$x \mapsto \text{DR}_n[\delta](x) = \frac{1}{1+n} \sum_{r=0}^n (R_A[\delta] \circ R_B[\delta])^r(x). \quad (3.1)$$

The number of double reflections, n , is one of the algorithm's hyperparameters. However, we will see that this algorithm only succeeds when the reflectors are themselves parameterized,

$$R_i[\delta](x) = (2 - \delta)P_i(x) - (1 - \delta)x, \quad (3.2)$$

and are made contractive with a positive setting of the hyperparameter δ . The original Douglas-Rachford iteration is recovered for $n = 1$ and $\delta = 0$ and will be referred to as $\text{DR}_1[0]$.

The idea behind (3.1) is that the double reflector acts as the identity when x is near a feasible point, and therefore the average of any number of double reflections fixes x . On the other hand, multiple ($n > 1$) applications of the double reflector might be better at ejecting x from a trap when it is not near a feasible point. Through elementary analysis and numerical experiments we will argue that there is an optimal δ^* such that when $\delta > \delta^*$, and the reflections are too contractive, the iterations become trapped at non-solutions, while for $\delta < \delta^*$ the iterate diffuses too freely to notice even the true solutions. The algorithm works best when δ is tuned to the dynamical transition point δ^* .

Hard feasibility problems, including the one we feature below, can often be formulated where one constraint set, say A , is discrete and the other, B , is a hyperplane. Traps arise when a point $a \in A$ is very close to B , that is, when the distance $\Delta = \|a - b\|$, to the proximal point $b = P_B(a)$ on the hyperplane, is very small. The local trapping/escaping behavior is analyzed by the dynamics just along the line defined by the proximal points $a \in A$, $b \in B$. With x as the (1D) coordinate along this line, and

$$P_A(x) = 0, \quad P_B(x) = -\Delta, \quad (3.3)$$

we find

$$\text{DR}_n[\delta](x) = \gamma x + c, \quad (3.4)$$

where

$$\begin{aligned} \gamma &= 1 - \frac{n(1-q) - q(1-q^n)}{(1+n)(1-q)} \\ q &= (1-\delta)^2 \\ c &= (1-\gamma) \left(\frac{1-\delta}{\delta} \right) \Delta. \end{aligned}$$

For comparison,

$$\text{DR}_1[0](x) = x + \Delta \quad (3.5)$$

represents a step-wise escape, where $O(1/\Delta)$ iterations are needed before x has changed by $O(1)$ in order that $P_A(x)$ is no longer the original point a of the trap.

Since $0 < \gamma < 1$ for $0 < \delta < 1$, iteration (3.4) looks problematic because there is always a (non-solution) fixed point:

$$x^* = \frac{c}{1-\gamma} = \left(\frac{1-\delta}{\delta} \right) \Delta. \quad (3.6)$$

However, (3.6) should be seen as instructions on the proper use of the algorithm. In any application there will be a smallest Δ that poses the greatest trapping risk. But by setting $\delta = \delta^* = O(\Delta)$, the fixed point x^* of the 1D dynamics is sufficiently far from the trap that $P_A(x^*)$ will be different from the original trapping point a . Since $c \sim n\Delta$ for $\delta \rightarrow 0$, a single iteration of DR_n is roughly the same as n iterations of DR_1 , although both schemes require n double-reflector computations.

Experiments with logical satisfiability. To illustrate the effect of the hyperparameter δ in a setting with potentially many traps, we turn to the logical satisfiability problem (SAT). In SAT we have a set C of *clauses* and a set V of *variables*. Thinking of these as vertices of a bipartite graph G , the search variables E in our constraint formulation correspond to edges $c \rightarrow v$, where $c \in C$ and $v \in V$. In the SAT interpretation, the variable-vertices v incident on a particular c in G correspond to the Boolean variables that participate in one clause of a logical formula in conjunctive normal form. The clause itself is a disjunction

$$y_c = \bigvee_{v \in V: c \rightarrow v \in E} n_{c \rightarrow v} \circ x_{c \rightarrow v} \quad (3.7)$$

where the x are Boolean variables, $n \circ$ specifies whether to apply negation, and y_c is the Boolean value of clause c . The object in SAT is to find an assignment to the x such that the conjunction

$$\bigwedge_{c \in C} y_c \quad (3.8)$$

is true. The set of Boolean variables $x_{c \rightarrow v}$ incident on the same v (but appearing in different clauses c) should all be equal. However, in the two-constraint formulation [9] to which we turn next, these are treated as independent in one of the constraints.

The two constraint sets live in a space of dimension $|E|$. Set A is discrete and imposes the truth of each clause (otherwise the conjunction (3.8) is false). We encode TRUE and FALSE for the Boolean variables as respectively $x = +1$ and $x = -1$ and use multiplication by $n = -1$ for negation:

$$\begin{aligned} A : \\ \forall c \rightarrow v \in E : x_{c \rightarrow v} \in \{-1, 1\} \\ \forall c \in C : +1 \in \bigcup_{v \in V: c \rightarrow v \in E} n_{c \rightarrow v} x_{c \rightarrow v} \end{aligned}$$

Because the A constraint imposes the discreteness of the Boolean variables we are free to use the following relaxed, continuous constraint for B :

$$\begin{aligned} B : \\ \forall v \in V : \exists \bar{x}_v \in \mathbb{R} : \\ \forall (c \in C : c \rightarrow v \in E) : x_{c \rightarrow v} = \bar{x}_v. \end{aligned} \quad (3.9)$$

We consider a hard instance of 3-SAT, where each clause involves exactly three variables and there are altogether $|V| = 500$ Boolean variables in the logical formula. The number of clauses $|C| = 2100$ was tuned so that a typical random instance has roughly even odds of being

satisfiable [10] (and this is true of our instance). All our results will be for iteration DR_3 , for which the number of double reflections ($n = 3$) is large enough that a transition in behavior with δ is easy to discern.

To visualize the results, we store the time series of the $|E|$ search variables in a matrix, where each row specifies a point in $\mathbb{R}^{|E|}$. We then find the principal component axes for this matrix and project each row onto the first two principal components to obtain a 2-dimensional plot of the search as a function of time. Since we are projecting points with root-mean-square distance $O(\sqrt{|E|})$, we also divide the principal components by $\sqrt{|E|}$ to normalize the length scale in the 2D plots. Alongside each PCA time series we provide the time series of the constraint error $\Delta = |P_A(x) - P_B(x)|$ for the points x generated by the DR_3 iteration.

The results are shown in Figure 1. When $\delta = 0.001$ (top plots of Fig. 1), the search jumps around aimlessly with large Δ and never finds a solution. We interpret this as small δ not being contractive enough: When δ is small, each reflection $R_i(x)$ is almost the same as the pure reflection $2P_i(x) - x$ and the algorithm never allows itself to fall into a basin of lower Δ . When $\delta = 0.02$ (bottom plots of Fig. 1), the algorithm quickly gets trapped on a non-solution and remains there for the rest of the search. Even though Δ is small, the algorithm never finds a solution. We interpret this as large δ being too contractive: the algorithm gets stuck in the first basin it finds, even though that basin likely does not contain a solution. The intermediate choice $\delta = 0.005$ (middle plots of Fig. 1) seems to be just right. The algorithm now appears to start exploring a basin once or twice but only stays for a few hundred iterations before wandering to another basin. After about 3×10^3 iterations it finds a basin that has a solution and converges toward it.

4. METRIC PARAMETERS

Metric parameters, unlike hyperparameters, are special for each intended application and should always be considered when there is more than one type of variable. Below we give two examples, both involving applications where the variables take discrete values and live on a network. As with hyperparameters, the settings of the metric parameters makes all the difference between an algorithm that never finds solutions and one that does so consistently.

Often a metric parameter will not have an obvious interpretation, or will have non-obvious interactions with the other metric parameters. Tuning these metric parameters can be done by hand and is informed by appropriate diagnostics that go beyond the standard “success rate” statistic. However, an automated procedure to expedite this process is desirable, especially when the number of metric parameters is large. We use a scheme where the current status of the search informs the rule for the parameter updates, and apply these updates adiabatically so as not to upend the fixed-point properties of the algorithm being used.

Our metric parameter update rule is based on the following heuristic. We want to prevent the algorithm from getting stuck on a partial solution, wherein some variables hardly change between the A and B projections while others are changing very much. We avoid this by giving a smaller metric parameter to the variables that are hardly changing, thereby lowering the penalty for changing them when the next projection comes, and vice versa for variables that change too much.

To be precise, suppose we partition the variables into k types, with metric parameters $\eta_1, \eta_2, \dots, \eta_k$. Let l_i denote the number of variables of type i , so that the complete variable vector can

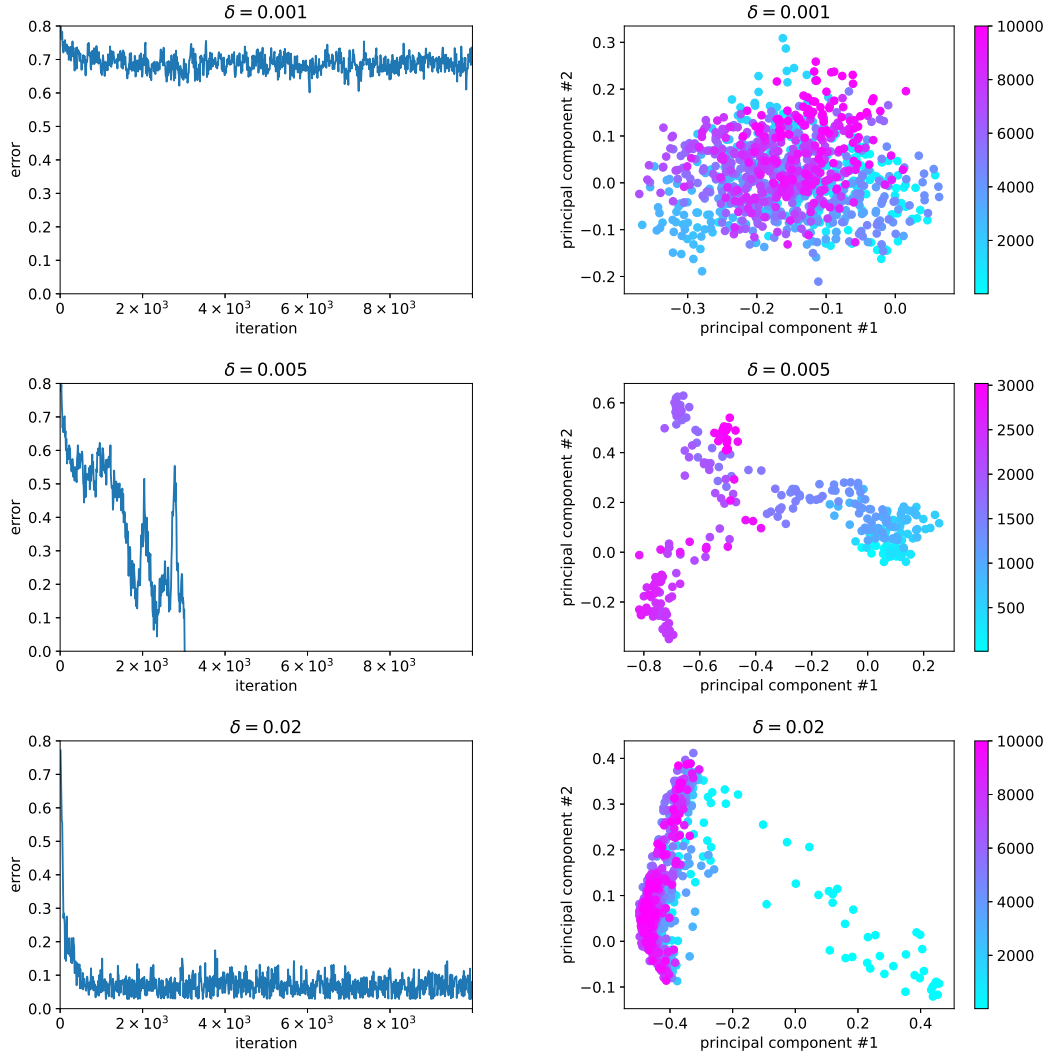


FIGURE 1. Plots of the constraint error $\|P_A(x) - P_B(x)\|$ (left column) and the iterate x (right column) of the DR_3 algorithm applied to an instance of 3-SAT. The three rows correspond to the reflectors being insufficiently contractive (top), too contractive (bottom), and a setting of δ in which the search succeeds (middle). The plots on the right show the iterate x projected into a 2D space by PCA. These data are plotted in increments of 10 iterations up to a maximum of 10^4 iterations, with the color bar indicating the iteration number.

be written as a concatenation $x = (x_1, x_2, \dots, x_k)$, where x_1 is a vector of length l_1 and so on. The projections are made using the distance function

$$d(x, x') = \sqrt{\sum_{i=1}^k \eta_i^2 \|x_i - x'_i\|^2}. \quad (4.1)$$

In each iteration, we compute the rms error

$$\varepsilon_i = \sqrt{\|P_A(x)_i - P_B(x)_i\|^2 / l_i} \quad (4.2)$$

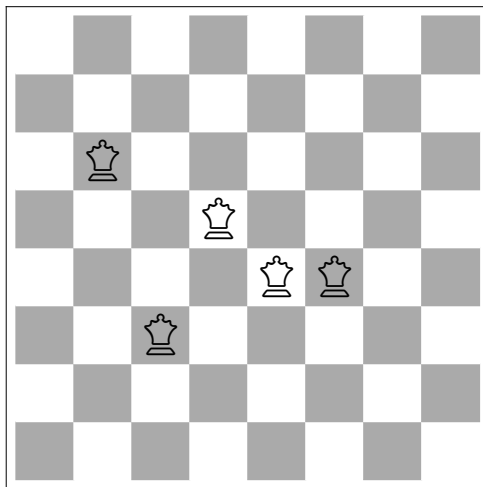


FIGURE 2. Five queens “dominating” the 8×8 chess board; that is, each unoccupied square is attacked by a queen. The domination number of the order 8 queens’ graph is 5 because this is not possible with fewer queens.

for each variable type. We then compare each ε_i to the average $\varepsilon = \sqrt{\frac{1}{k} \sum_i \varepsilon_i^2}$ and adjust the metric parameters according to

$$\eta_i \rightarrow \eta_i (1 + \alpha (\varepsilon_i / \varepsilon - 1)). \quad (4.3)$$

Alternatively, since only the relative weights of the variable types matter, one can set $\eta_1 = 1$ and take

$$\eta_i \rightarrow \eta_i (1 + \alpha (\varepsilon_i / \varepsilon_1 - 1)) \quad (4.4)$$

for $i > 1$.

Automatically updating the metric parameters in this fashion encourages the smaller ε_i ’s to become larger and vice versa, which leads to the ε_i ’s being highly correlated, which in turn generally leads to more successful searching. This approach also replaces the problem of tuning some (possibly large) number of metric parameters with the simpler question of choosing a value of α . One must have $\alpha \ll 1$ in order to make the metric parameter updates adiabatic and thereby preserve the local convergence properties of the algorithm. One also wants $\alpha \gg 1/N$, where N is the total number of iterations to be run, so as to accomplish the desired tuning within the intended length of the run. Accordingly, for large N there can be a rather generous range of α that will work.

Experiments. For the following experiments we use the relaxed Douglas-Rachford algorithm (2.1). In each example we first choose a value of the hyperparameter β that works for that particular problem ($\beta = 0.5$ for the dominating sets example, $\beta = 0.8$ for the Boolean generative networks example), then choose a challenging instance of the problem and demonstrate the benefits of tuning the metric parameters while keeping the hyperparameter fixed.

Experiments with dominating sets. Consider a graph G with vertices V and (undirected) edges E . A subset $D \subset V$ dominates G if for every vertex $i \in V$ either $i \in D$ or there exists an adjacent vertex j such that $(i, j) \in E$ and $j \in D$. Finding dominating sets of minimum size $|D|$ is a well known NP-hard problem. Chess players will recognize the configuration shown in Figure 2

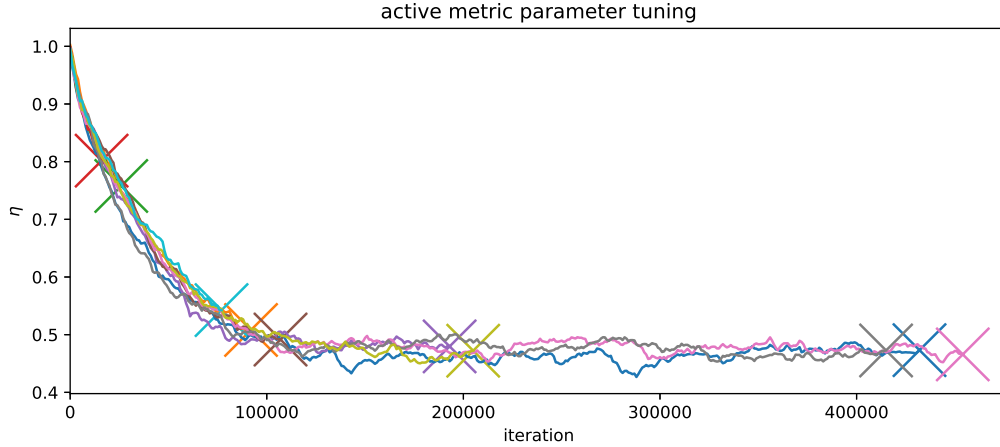


FIGURE 3. Time series of the metric parameter η when tuned automatically in ten trials of finding a dominating set for the order 12 queens' graph. Each curve terminates when the algorithm finds a solution, demarcated by an X. Note that the tuning consistently leads to $\eta \approx 0.5$.

as an instance of a dominating set. Here the squares of the board are graph vertices and two squares are “connected” by an edge if a queen placed on one attacks the other. The *domination number* of this particular board/graph is $|D| = 5$ because the five queens attack all the other squares and this is not possible with fewer queens.

That a vertex may be dominated either by itself or an adjacent vertex calls for two types of variable in a constraint formulation. A metric parameter should be introduced to control their relative “weight.” Our formulation uses vertex variables y_i , $i \in V$ and two variables for each edge $(i, j) \in E$: $x_{i \rightarrow j}$ and $x_{j \rightarrow i}$. We denote the set of doubled edges E_2 . One can think of $x_{i \rightarrow j}$ as a copy of vertex i that vertex j uses to express its domination status. Since there are only two variable types, a single metric parameter η suffices to characterize the weight of the vertex variables relative to the edge variables. Constraint *A* demands that every vertex is either self-dominating or is dominated by at least one adjacent vertex via an incident edge, with at most $|D|$ vertices being self-dominating, while constraint *B* demands that all edge variables agree with their associated vertex variable:

A :

$$\forall j \rightarrow i \in E_2: \quad x_{j \rightarrow i} \in \{0, 1\},$$

$$\forall i \in V: \quad y_i \in \{0, \eta\} \quad \wedge \quad y_i/\eta + \sum_{j \rightarrow i} x_{j \rightarrow i} \geq 1,$$

$$\sum_{i \in V} y_i/\eta \leq |D| \quad ,$$

B :

$$\forall j \rightarrow i \in E_2: \quad x_{j \rightarrow i} = y_j/\eta.$$

Projections to both constraint sets is an easy computation. Constraint *A* is slightly non-local in that all the vertices need to be ranked by their distance to $y_i = \eta$ over $y_i = 0$ when selecting the optimal subset of size $|D|$.

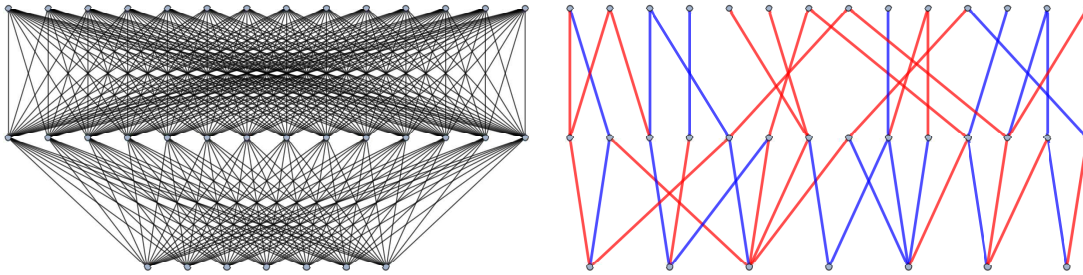


FIGURE 4. Network architecture (left) that takes 7 Boolean inputs and outputs 14 Boolean data; there is also an intermediate layer that holds 14 Boolean values. The trained BGN (right) is a logical circuit that uses relatively few of the available network edges as wires. All the nodes not in the input layer apply OR to the wires incident from below. Training also determines the placement of the NOT gates, which are indicated by red wires.

Figure 3 plots the progress of the metric parameter as the algorithm searches for a dominating set of size $|D| = 6$ for the queens’ graph of order 12. Each curve in the figure terminates when the algorithm finds a solution. The average number of iterations required for this collection of trials was about 2×10^5 ; for comparison, the same algorithm with no metric parameter tuning often fails to find a solution after 10^6 iterations. Note that the metric parameter consistently tunes itself to a value near 0.5. For other problems the optimal parameter is in general something else, but the benefit of letting the weights tune themselves is that the user need not change any settings in order to solve another instance (apart from increasing the maximum number of iterations for harder instances).

Experiments with Boolean generative networks. Our second example of automated metric parameter tuning is unsupervised machine learning with a Boolean generative network, or BGN [11]. The data in this application consist of a set of D Boolean strings of length N , and the network is tasked with discovering a Boolean circuit that generates the strings from a smaller number $M < N$ of Boolean “latent variables” whose values for each data string are unknown. Figure 4 compares a network before and after training. Nodes of the network are arranged in layers and initially each node can potentially receive input from any node in the layer below. However, the data come with the promise or hypothesis that they can be generated with only NOT and 2-input OR gates. Through training the network must therefore discover which of the many edges are utilized in the circuit, that is, the “wires” of the circuit, and whether the Boolean value is to be negated when traversing the wire.

The truth value at a node i of the BGN is encoded by a variable y_i at that node and also by copies of that truth value on all its out-edges, $x_{i \rightarrow j}$. These two variable types have the same interpretation they had in the dominating set application and serve to localize the constraints. However, by the uni-directional nature of the BGN logic, there is no need to have a second variable on each edge. Just as with dominating sets, the semantic equivalence of the x and y variables does not imply metrical equivalence and we control their relative scale with metric parameters θ and η .

The relevance of metric parameters in BGNs is made especially obvious when we also consider the variables $w_{i \rightarrow j}$ used to encode whether an edge $i \rightarrow j$ of the network is a wire and if

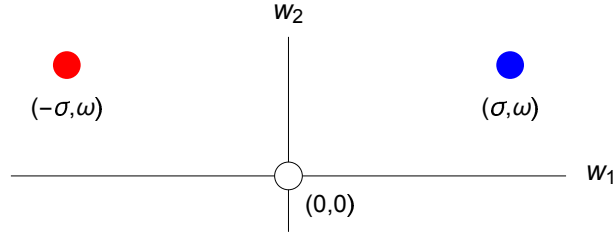


FIGURE 5. A 2D space (w_1, w_2) is required to encode the three possible states of edges in a BGN. The red and blue points correspond to edges utilized as wires with and without negation; the open circle encodes the absence of a wire. Two metric parameters, σ and ω , define the isosceles geometry of the states.

so, its negation state. To encode the three states of an edge as three points we should use a 2D space to make available the most general metrical relationship among the states. Not only is the wire-status of an edge semantically distinct from the truth states it operates on, the existence of a wire (on the edge) should have independence, metrically, over its two negation states. These considerations are addressed by encoding the wire states by the vertices of an isosceles triangle as shown in Figure 5. The metric parameter ω now controls the distance between presence and absence of a wire, while σ controls the distance between the presence and absence of a NOT.

In order to solve the problem we create a copy of the network for each of the D data strings. One of the constraints is that the choice of wire states is the same across all copies of the network. The states (truth values) of the nodes will in general be different, as they depend on each instantiation of the network through the data string. It often happens that certain nodes and edges in the network are more important than others. For instance, nodes in different layers or having different in- or out-degrees could play markedly different roles. It is natural then to let the metric parameters be different for every node and edge in the network, promoting ω , σ , θ , and η to $\omega_{i \rightarrow j}$, $\sigma_{i \rightarrow j}$, $\theta_{i \rightarrow j}$, and η_i . Finally, one could also argue that the D data strings have differing inherent difficulty and deserve suitably tuned metric parameters applied to their copies of the network. Instead of a single $\omega_{i \rightarrow j}$ parameter for edge $i \rightarrow j$ there would then be parameters $\omega_{d, i \rightarrow j}$ for $d = 1, \dots, D$ and similarly for the other variable types. Below we refer to these refinements of metric parameter tuning as by “type,” “network location,” and “data item.”

We compared the different degrees of metric parameterization on a synthetic data set generated by the circuit in Figure 4 with $M = 7$ inputs and $N = 14$ outputs. For training we used all $D = 87$ unique data strings generated by this circuit and initialized the variables (on nodes and edges of the complete architecture) to random values selected in the ranges of the four “type” parameters (ω , σ , θ , η). Solutions (circuits) were only required to generate all D data strings for some setting of the M inputs. Typically the solution circuits additionally generated strings not among the D data strings, though never a set of size 2^M .

Figure 6 plots the time series of the constraint errors for each of the four variable types — ϵ_{w_1} , ϵ_{w_2} , ϵ_x , ϵ_y — for each of the four degrees of metric parameter tuning. The top left plot is for the naive choice of metric parameters with no tuning; that is, we set $\sigma = \omega = \theta = \eta = 1$ and take $\alpha = 0$ in (4.3). The constraint error for w_2 quickly drops to zero, but the others stay at roughly constant nonzero values. Clearly this search is stuck on a non-solution. In the top right plot, we again initialize the metric parameters to 1 but now we set $\alpha = 10^{-4}$ to allow the four parameters to be slowly tuned as the search progresses. One can see that the search does

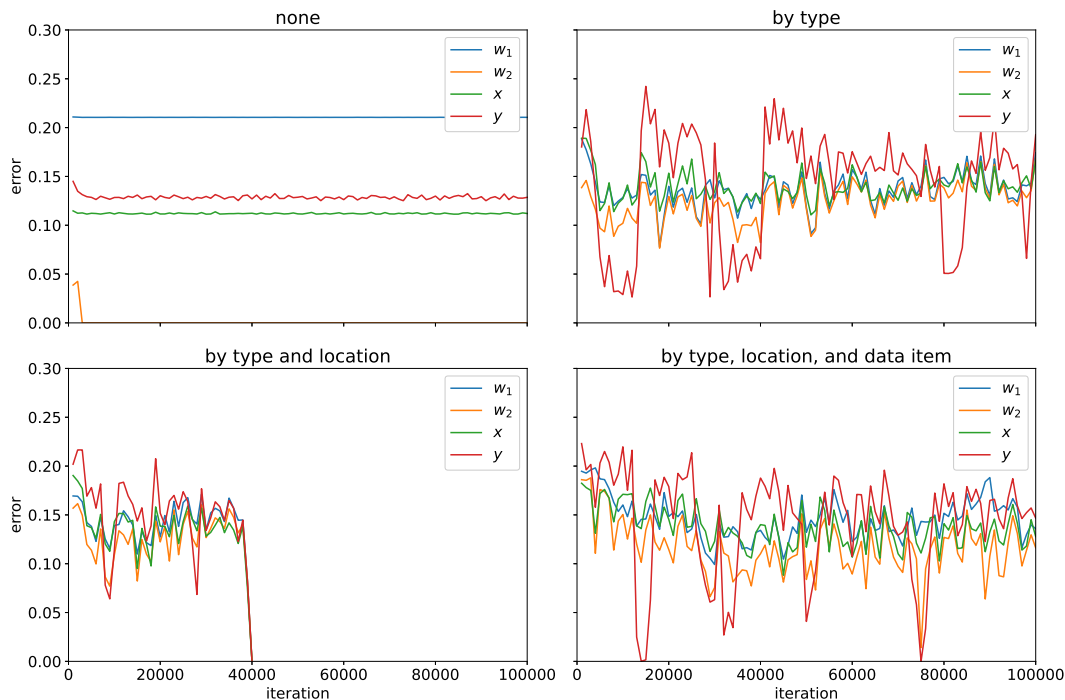


FIGURE 6. Time series of the constraint errors for the BGN problem with four levels of metric parameter tuning. *Top left*: no tuning. *Top right*: tuning by variable type. *Bottom left*: tuning by type and location within the network. *Bottom right*: tuning by type, location, and data item. The four errors in each plot are those of the four variable types described in the text.

not get stuck the way it did with $\alpha = 0$. In the bottom left plot, we promote ω to $\omega_{i \rightarrow j}$, σ to $\sigma_{i \rightarrow j}$, and so on, to allow the metric parameters to vary also by location within the network. We still initialize the parameters to 1 and use $\alpha = 10^{-4}$. This search is even more effective, with the four constraint errors strongly correlated. It terminates early because it finds a solution after about 4×10^4 iterations. Finally, in the bottom right we go one step further, promoting $\omega_{i \rightarrow j}$ to $\omega_{d, i \rightarrow j}$, $\sigma_{i \rightarrow j}$ to $\sigma_{d, i \rightarrow j}$, and so on, to allow the metric parameters to vary by data item as well. As always we initialize the metric parameters to 1, and we still use $\alpha = 10^{-4}$. The search is better than it was with no tuning, but not much better than tuning by type and not as effective as tuning by type and location.

Even though the four plots in Figure 6 only show a single example of a search for each level of tuning, the examples chosen are representative: Tuning by type and location consistently outperforms the other approaches. We have also tried other tuning combinations, such as by type and data item but not location, and the performance is similar to that of tuning by type, location, and data item. Evidently adding more metric parameters is not always better. Tuning by location was helpful in this example, but tuning by data item was not.

One possible interpretation of these results is that metric parameters have tangible effects only when they target systematic or structural properties of the variables. The nodes of the BGN distinguish themselves by their in- and out-degrees, and also their distance from data constraints (imposed only at the output layer). We should therefore expect a metric-tuning benefit based on

network location just as for the more obvious case of variables distinct by type (node vs. edge). In the case of variables differing only by the data index, the structural bias is much weaker. For most of these variables the structural difference is only indirect, through the fixed-value data constraints at the output nodes.

An alternative viewpoint is that metric parameters facilitate symmetry breaking behavior. For example, it may be important that nodes within the same layer are able to develop unique characteristics, even while the associated node and edge variables have a permutation symmetry. Likewise, some data items might pose a greater challenge to the circuit than others, and the metric parameters of their associated variables would serve to break that form of permutation symmetry. Although our survey of results is far from comprehensive, the absence of a noticeable benefit from tuning by data index leads us to believe that the structural hypothesis is better supported than symmetry breaking.

5. CONCLUSIONS

We suspect that quite a few applications of iterative projection methods on nonconvex problems may have been abandoned because of a failure to recognize a sensitivity to parameters. Even in the case of hyperparameters, a setting in a range that is “safe” with respect to local convergence (where the constraints may be approximated as convex) overlooks the fact that these parameters also have a profound effect on the global characteristics of the search. We saw an example of this in the Douglas-Rachford generalization of section 3, where the contractivity δ needs to be tuned to a sweet spot for effective search. The tuning of metric parameters is equally important in applications where there is a rescaling freedom among variables not subject to symmetry. Such applications, without the translation or permutation symmetries of phase retrieval or a sudoku puzzle, are relatively new for iterative projection methods. Recognizing the role of the metric in such applications, and not arbitrarily assigning 1 as the relative scale, is an important first step. One can tune the metric parameters by hand, but here we have introduced a method for updating them automatically based on constraint errors. This approach is particularly useful when there are many metric parameters to tune.

Acknowledgments

The authors thank Avinash Mandaiya for noticing the two variable types in the dominating set problem and Jim Sethna for useful conversations.

REFERENCES

- [1] V. Elser, The complexity of bit retrieval, *IEEE Transactions on Information Theory* 64.1 (2017), 412-428.
- [2] F.J.A. Artacho, J.M. Borwein, and M.K. Tam, Global behavior of the Douglas–Rachford method for a non-convex feasibility problem, *Journal of Global Optimization* 65.2 (2016), 309-327.
- [3] V. Elser, Matrix product constraints by projection methods, *Journal of Global Optimization* 68.2 (2017), 329-355.
- [4] F.J.A. Artacho, R. Campoy, and M.K. Tam, The Douglas–Rachford algorithm for convex and nonconvex feasibility problems, *Mathematical Methods of Operations Research* 91.2 (2020), 201-240.
- [5] J.R. Fienup, Phase retrieval algorithms: a comparison, *Applied optics* 21.15 (1982), 2758-2769.
- [6] V. Elser, T.-Y. Lan, and T. Bendory, Benchmark problems for phase retrieval, *SIAM Journal on Imaging Sciences* 11.4 (2018), 2429-2455.
- [7] F.J.A. Artacho, J.M. Borwein, and M.K. Tam, Recent results on Douglas–Rachford methods, *Serdica Mathematical Journal* 39.3-4 (2013), 313-330.

- [8] V. Elser, Learning without loss, arXiv preprint arXiv:1911.00493 (2019).
- [9] S. Gravel, and V. Elser, Divide and concur: A general approach to constraint satisfaction, *Physical Review E* 78.3 (2008), 036706.
- [10] D. Mitchell, B. Selman, and H. Levesque, Hard and easy distributions of SAT problems, *AAAI Vol. 92* (1992).
- [11] V. Elser, Reconstructing cellular automata rules from observations at nonconsecutive times, arXiv preprint arXiv:2012.02179 (2020).